ELSEVIER

Journal of Materials Processing Technology 174 (2006) 286–292

Journal of Materials Processing Technology

www.elsevier.com/locate/jmatprotec

# On the FE codes capability for tool temperature calculation in machining processes

L. Filice [a,*], D. Umbrello [a], S. Beccari [b], F. Micari [b]

[a] *Department of Mechanical Engineering, University of Calabria, Rende, Italy*

[b] *Department of Mechanical Technology, Production and Management Engineering, University of Palermo, Palermo, Italy*

Received 6 January 2005; received in revised form 31 January 2006; accepted 31 January 2006

**Abstract**

The applications of numerical simulation to machining processes have been more and more growing in the last years: today a quite effective predictive capability has been reached, at least as far as global cutting variables (for instance cutting forces) are concerned. On the other hand, the capability to predict local cutting variables (i.e. pressure on the tool, temperature distribution, residual stresses in the machined surface) has to be heavily improved and verified. At the same time, effective experimental procedures for validating numerical results have to be developed.

In this work two different approaches were implemented for temperature measuring: a thermocouple based approach and a thermographic analysis were developed. As well the effectiveness of a couple of typologies of numerical simulation was investigated; the former was a 2D fully thermo-mechanical analysis, the latter a 3D pure thermal one.

The results of the study permit to assess that a thermo-mechanical simulation does not permit a satisfactory temperature prediction, while an integrated approach including analytical models and pure thermal FE simulations promises relevant advantages.


*Keywords:* Temperature in machining; Cutting; FEM

## 1. Introduction

Conventional machining and, in the last years, hard turning processes, have to be considered among the most important manufacturing technologies. Due to the nonlinear nature of metal cutting and the complex coupling between deformation and temperatures fields, a reliable evaluation of the temperature distributions during the machining process is very important.

The mechanical work required to remove material during machining is mainly converted into thermal energy that increases the temperature of the workpiece, chip and cutting tool. High cutting tool temperatures affect material properties leading to a decreasing of tool life, determining, as well poor surface finishing.

The determination of cutting temperature distribution is technically difficult and previous researches did not provide sufficiently accurate temperature data, as mentioned by Shaw [1], Boothroyd [2], Kalpakjian [3] and Trent and Wright [4]. The use of numerical simulation may constitute a breakpoint but it effectiveness as to be proved through accurate tests. Experimental data on cutting temperature distribution are required to achieve a better understanding of the influence of the main parameters including cutting tool materials, coatings, cutting speed, and workpiece material.

The first attempt in the technical literature is probably due to Boothroyd [5], who used infrared film to map out steady-state temperatures in turning. Chao et al. [6] used a PbS photoconductive cell to measure temperatures on the flank face of cutting tool. Prins [7] used a pyrometer to measure rake face temperatures. Lezanski and Shaw [8] used the intrinsic thermocouples method to determine temperature at the tool–chip contact. Furthermore, Ay et al. [9] used an embedded fine gauge thermocouple in a cutting tool to map out the temperature. Stephenson [10], Muller et al. [11], M'Saoubi et al. [12] and Davies et al. [13,14] used thermo-video cameras to measure temperatures in the deformation zone behind the cutting tool tip.

* Corresponding author at: Ponte Pietro Bucci, 45 C, Rende (CS) 87036, Italy. Tel.: +39 0984494608; fax: +39 0984494673.

*E-mail addresses:* l.filice@unical.it (L. Filice), d.umbrello@unical.it (D. Umbrello), beccari@dtpm.unipa.it (S. Beccari), micari@dtpm.unipa.it (F. Micari).

*URL:* www.unical.it, www.unipa.it.

0924-0136/$ – see front matter © 2006 Elsevier B.V. All rights reserved.
doi:10.1016/j.jmatprotec.2006.01.012

It is worth outlining that many of these studies were carried out at very low cutting speeds. Miller et al. [15] developed a suitable experimental technique utilizing modern digital infrared thermometry to solve several difficulties linked to the measurement of cutting temperature distribution during orthogonal machining. Their data have a resolution and accuracy not previously obtained and the developed technique was applied under ordinary shop floor conditions, using a cutting speed up to 3.4 m/s for an AISI 1025 workpiece.

In a very modern approach, experimental temperature data are necessary to validate and improve computational models, such as finite element method, capable of predicting tool temperature and modelling mechanisms directly related to heat generation, like the tool wear. The models, whose reliability must be assessed using experimental data, can be used to properly select the cutting tool materials and coatings, design the tool geometry and fully optimize the machining processes. These results became strategic for industry, permitting to extend cutting tool life, reducing production costs, potentially increasing the production rates and improving part quality.

Numerical simulation permits to calculate complete temperature distributions; unfortunately, only few studies have developed methods able to [15,16] generate acceptable errors.

In this paper two different approaches are presented in order to measure the temperature distribution into a cutting tool. The former is based on the embedded thermocouples into the tool, the latter on the use of a thermographic analysis, based on the revealing of the infrared emission of an in-process tool.

All the tests were carried out on steel tubes machined at conventional cutting speed in orthogonal conditions.

As well, two typologies of numerical simulation were performed: firstly a 2D plane strain fully thermo-mechanical simulation was run to predict the temperature history in the tool. Actually, such model does not permit the achievement of steady-state conditions unless properly modified thermal parameters are introduced. The simulation cutting time is, in fact, about 2 or 3 orders lower than the time necessary to reach steady-state conditions due to the required CPU time.

The alternative approach is based on the preliminary evaluation of the thermal flow on the tool and, then, on the simulation of the pure thermal evolution into the insert. In this way, the simulated time can be equal to the experimental one, giving very accurate predictions. Of course, in this case the main problem is determination of the boundary conditions and, in particular, of the heat flux in the tool during the process.

All these aspects are diffusely discussed in the following sections.

## 2. Experimental approach

As above-mentioned, two experimental methodologies were utilized for the evaluation of temperature distributions: embedded thermocouples and a high resolution thermographic system. In both the cases, machining operations were carried out on AISI 1045 tubes (diameter 100 mm, thickness 3 mm). The turning parameters were 0.1 or 0.2 mm/rev, as feed rate, and 125 or 200 m/min as cutting speed. An uncoated carbide insert (94% WC, 6% Co), supplied by Vandurit, was used as tool. In the former class of the experiments two thermocouples were embedded in the insert, while in the latter the lateral surface of the insert was properly ground to make effective the thermographic analysis.

### 2.1. Embedded thermocouple system

Two holes were bored in the insert by means of an EDM machine, at different distance (0.5 and 0.9 mm, respectively) from the rake face. K-type thermocouples were properly forced into the hole to obtain the local temperature [17]; the position of thermocouples is shown in Fig. 1.

The ready-to-use tool and the machining set-up are shown in Fig. 2a and b.

Some of the experimental results provided by thermocouples are reported in Fig. 3. The steady temperature 0.5 mm below the rake face was about 500 °C, whilst temperature 0.9 mm below the rake face was about 450 °C for cutting speed and a feed rate equal to 200 m/min and 0.2 mm/rev, respectively.

In good agreement with the expectations, the temperature gradient was higher for the thermocouple at 0.5 mm. Anyway, in both cases, about 20 s were necessary to reach the final steady temperature.

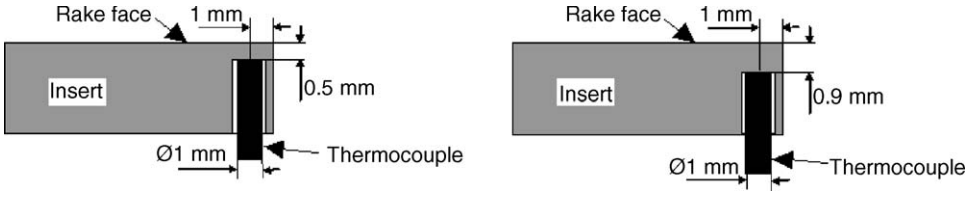


Fig. 1. Thermocouples positioning into the tool body.

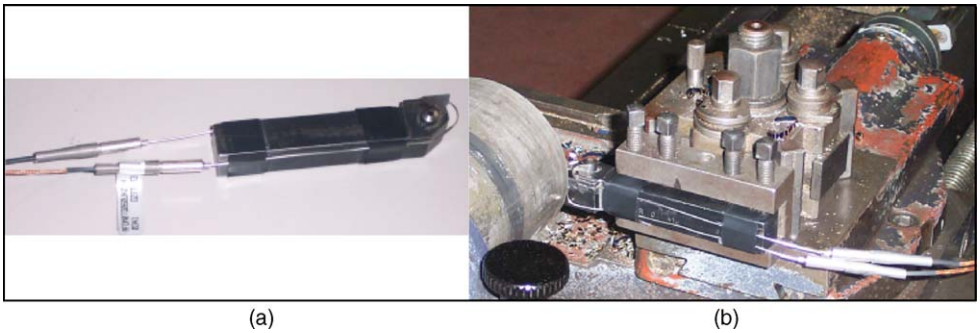


Fig. 2. (a) Ready-to-use tool and (b) machining set-up.

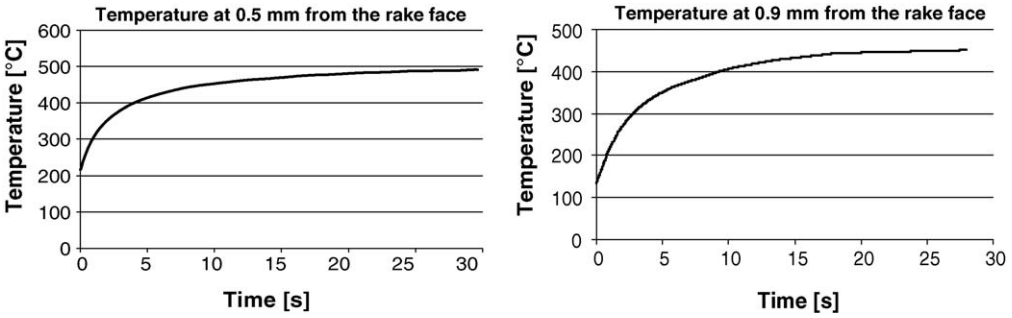


Fig. 3. Temperature diagrams of thermocouples ($V = 200$ m/min, $f = 0.2$ mm/rev).

Table 1
Experimental results

| Cutting speed (m/min) | Feed rate (mm/rev) | Experimental steady temperature (°C) |
|---|---|---|
| 122 | 0.1 | 345 |
| 122 | 0.2 | 475 |
| 200 | 0.1 | 365 |
| 200 | 0.2 | 500 |

Furthermore, in order to investigate the effects of the turning parameters, other experiments to measure the local cutting temperature at the varying of the feed rate and cutting speed were performed. In these cases, only one thermocouple at distance of 0.5 mm from the rake face was embedded in the uncoated carbide insert to reduce discontinuities in the tool material. The experimental steady-state results deriving from the measurements are shown in Table 1.

The obtained results are in good agreement with values reported in literature. This technique, anyway, is able to supply temperature measures only in few points inside the tool. For this reason the thermographic system was utilized as well to achieve other relevant data.

### 2.2. High resolution thermographic system

Machining experiments were carried out fixing the same conditions as above. The experimental set-up is shown in Fig. 4a and b.

The utilized tool was prepared by grinding the flank surface (Fig. 4b). In this way the thermocamera is able to acquire the thermal signal from an "optimal" surface whose versor is adjacent to the camera axis (see also Figs. 5 and 10). An high resolution thermographic system was utilized enabling to generate thermal maps of the tool flank at a distance of 1 mm from the chip flow zone (see again Fig. 4b). The thermographic technique, opposite to thermocouples and other similar methods, is a non-contact system and therefore does not influence the measured phenomenon. However, the thermographic system requires a long and complex calibration and the results fully depend on many factors such as the surface conditions of examined object and environmental absorption and reflection of infrared radiations [15,16].

Table 2
Thermographic system technical specifications

| | |
|---|---|
| IR detector | MCT |
| Operating wavelength range | 2–5 μm |
| Temperature resolution (30 °C object temperature) | ±0.12 K |
| Temperature measuring range | −10 to +1200 °C |
| Absolute accuracy of temperature measurement at an ambient temperature of 22 ± 2 °C and $\varepsilon = 1$ | ±2 K up to 100 °C, otherwise ±1% of full-scale value each |
| Scanned object field | 30° (H) × 20° (V) |
| Geometrical resolution | 3 mrad |
| Pixel per image | 360 × 240 |
| Object distance | 0.2 m to ∞ |
| A/D conversion | 16 bit |
| Optical zoom levels | 5 |

It is well known that all the materials emit radiant energy as a consequence of their temperature. The linkage between radiated energy $J$ (specific thermal power (W/m$^2$)) and temperature $T$ (K) is given by the Stefan–Boltzmann law:

$$J = \varepsilon \sigma T^4 \quad (1)$$

being $\varepsilon$ the emissivity of the surface of the object and $\sigma = 5.675 \times 10^{-8}$ W/m$^2$ K$^4$ the Stefan–Boltzmann constant. Emissivity ($\varepsilon$) is defined as the ratio of the energy radiated by an object at an assigned temperature versus the energy emitted by a perfect radiator, or "black body", at the same temperature.

An accurate calibration of the thermographic system was carried out to find the emissivity value of the tool material, according to the following simple procedure. The insert was placed in a controlled temperature furnace and some thermographic images were taken at different temperatures. The emissivity of the material was calibrated by means of an inverse approach and supplied to the camera. The tool emissivity did not significantly change with temperature and its value was determined equal to $\varepsilon = 0.8$. Technical specifications of the utilized thermographic system are reported in Table 2.

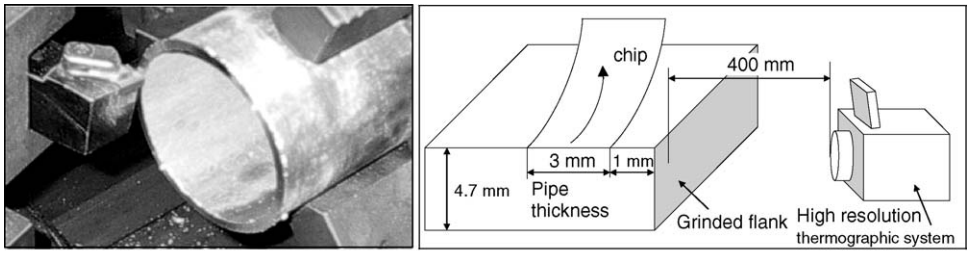


Fig. 4. (a) Experimental set-up and (b) scheme of thermographic measurement.

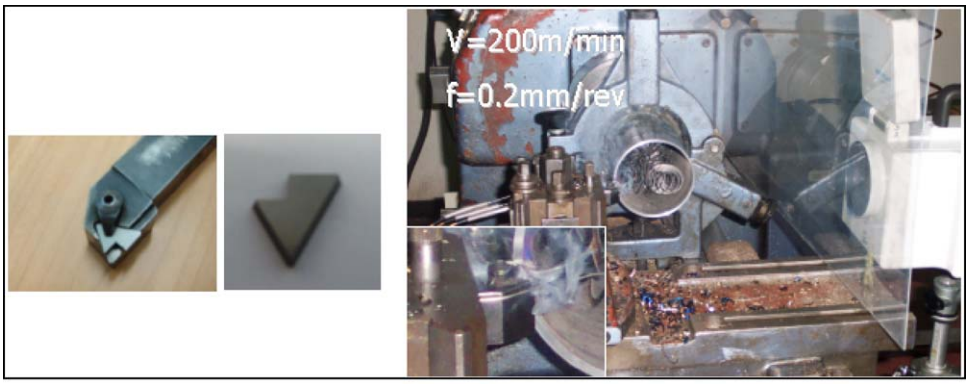


Fig. 5. (a) Utilized tool and (b) the equipment.

Fig. 5 shows the utilized tool and the equipment used in the machining operation, while Fig. 6 reports the result obtained by high resolution thermography system for cutting speed and a feed rate equal to 200 m/min and 0.2 mm/rev, respectively.

## 3. Numerical analysis

The cutting process was modelled utilizing the SFTC-Deform® finite element code. As mentioned both a 2D plane-strain coupled thermo-mechanical analysis and a pure thermal 3D analysis were carried out.

### 3.1. Case 1: 2D thermo-mechanical analysis

The workpiece was initially meshed with 5000 isoparametric quadrilateral elements although, during the simulation, the remeshing algorithm increased this number up to 7000. The tool, modelled as rigid, was meshed and subdivided into 1000 elements.

According to the experiments the cutting speed was set equal to 122 and 200 m/min while the feed was set equal to 0.1 and 0.2 mm/rev. The rake angle was $\gamma = 0^\circ$ while the tool fillet radius was equal to 0.02 mm, according to the utilized tool. Fig. 7 shows the undeformed mesh for both the tool and the workpiece at the beginning of the simulation.

Due to the heavy strain, strain rate and temperature conditions, a particular attention was paid for rheological behavior modelling. According to previous works, the Lin and Lin [18] material model was implemented.

As far as friction modelling is concerned, a simple model based on the constant shear hypothesis was utilized. The shear factor was kept equal to $m = 0.65$ [19], which permitted a satisfactory prediction of cutting forces and chip geometry are concerned.

A particular attention was paid on the thermal parameters in order to properly investigate temperature increase, due to plastic work in the primary shear zone and to friction on the rake face (secondary shear zone), and the heat transfer phenomena. Table 3 summarizes the most relevant thermal parameters used

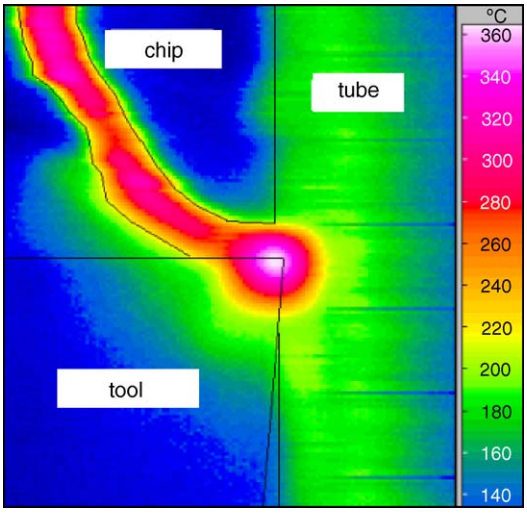


Fig. 6. Experimental temperature distribution obtained by high resolution thermography system.

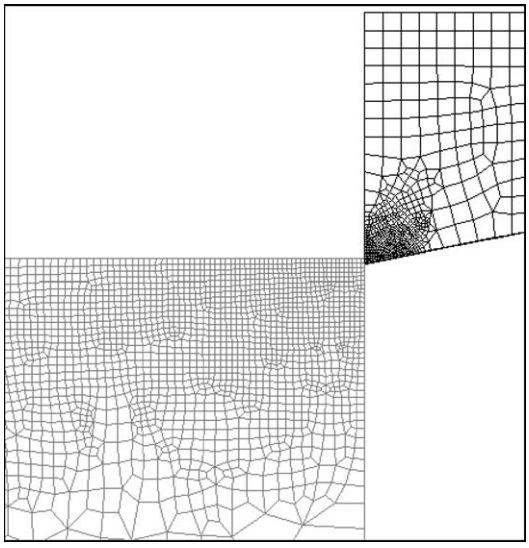

Fig. 7. The undeformed mesh.

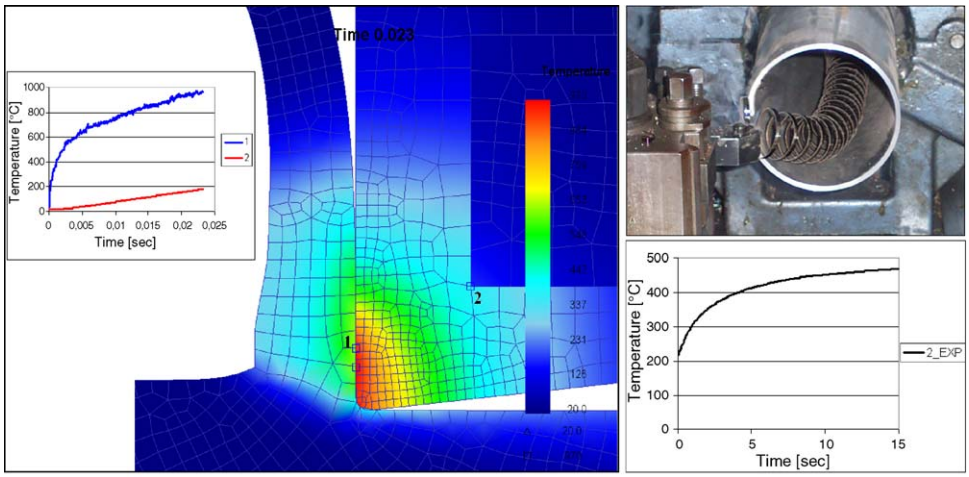


Fig. 8. Case $V = 200$ m/min, $f = 0.2$ mm/rev: (a) numerical results and (b) experimental results.

Table 3
Thermal parameters utilized in the model

| Parameter | Value | Unit |
|---|---|---|
| Workpiece (AISI 1045) | | |
| Heat capacity | $3.81 \times 10^6$ | J/m$^3$ K |
| Thermal conductivity | 50 | W/m K |
| Emissivity | 0.8 | |
| Tool (Vandurit G1) | | |
| Heat capacity | $2.95 \times 10^6$ | J/m$^3$ K |
| Thermal conductivity | 80 | W/m K |
| Emissivity | 0.45 | |
| Workpiece–tool interface | | |
| Heat transfer coefficient | 30 | kW/m$^2$ K |

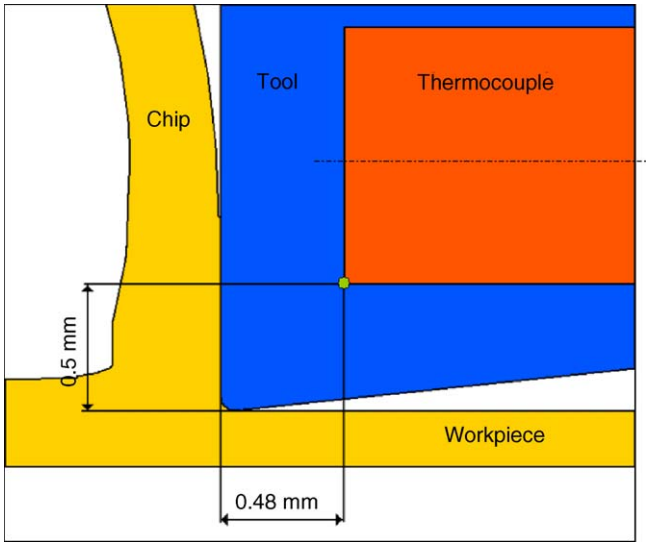


Fig. 9. Thermocouple position.

in the simulations for both AISI 1045 workpiece material and the uncoated carbide tool.

Some interesting results are shown in Fig. 8a and b. In the former instants of the process, the simulation follows process mechanics, but the temperature increases with a different law respect to the experiments.

In the simulated time no steady-state conditions can be reached into the tool. At the investigated cutting speeds, actually close to the conventional values, few milliseconds can be properly simulated according to the available computer technology, while 10–20 s are necessary as shown by the experiments.

Some researchers proposed to reach early steady-state conditions through an arbitrary tuning of the global heat transfer coefficient. In this way the heat flux between tool and chip sharply increases, determining a quicker thermal equilibrium. Actually, since the heat capacity of the tool is lower than the workpiece one, part of the heat flux generated by friction into the tool moves toward the chip, reducing tool temperature. In addition, the contribute on heat generation due to the plastic work is not relevant for the whole equilibrium, since few millisecond of simulation are not enough to permit its transfer to the tool.

Table 4
Comparison of the numerically and experimentally obtained temperature distributions

| Cutting speed (m/min) | Feed rate (mm/rev) | Experimental steady temperature (°C) | Predicted transient temperature (°C) |
|---|---|---|---|
| 122 | 0.1 | 345 | 62 |
| 122 | 0.2 | 475 | 85 |
| 200 | 0.1 | 365 | 105 |
| 200 | 0.2 | 500 | 156 |

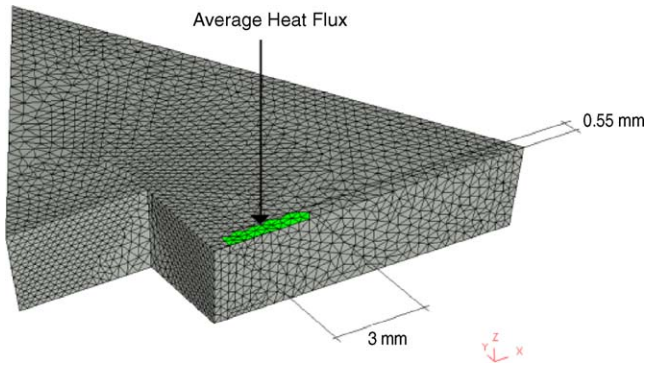


Fig. 10. The initial 3D mesh and the thermal boundary conditions.

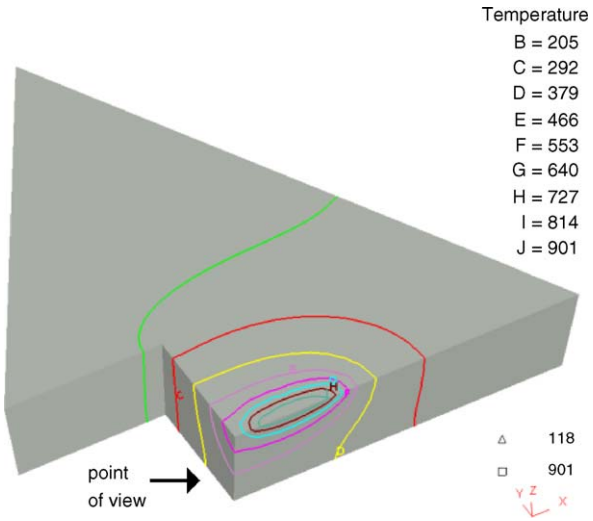


Fig. 11. Predicted temperature distributions: $V = 200$ m/min, $f = 0.2$ mm/rev.

Furthermore, from a pure scientific point of view, it is not very correct to set the global exchange coefficient value by an inverse approach, such parameters, in fact, represents a physical phenomenon and has a precise value, experimentally determinable.

Table 4 reports the comparison between the experimentally measured temperatures and the maximum predicted values for the thermocouple closer to the rake face (Fig. 9).

Some other numerical tests were carried out increasing the simulation time, i.e. extending the length of the workpiece. Although, the tests were carried out on a powerful dual processor 2.8 GHz CPU with 2 GB RAM no steady-state conditions were reached.

### 3.2. Case 2: integrated analytical-3D thermal approach

In this case only the insert was modeled by means of 50,000 solid elements (Fig. 10).

The question is now how to model the heat generation due to the process mechanics. According to the available knowledge, it was assumed that a reasonable percentage of the total mechanical work is transformed into heat that moves towards the tool. In the case cutting speed $V = 200$ m/min and feed $f = 0.2$ mm/rev the average heat flux, supposed uniformly applied on the chip-rake face contact area, was fixed equal to 33,000 kW/m$^2$ K; namely the 3% of the total power calculated on the basis of the measured cutting force and cutting speed. Fig. 11 shows the FEM temperature distribution in the tool after 15 s, i.e. after the achievement of the steady-state conditions.

FEM simulation provided also the maximum temperature, equal to about 900 °C, at the interface between chip and rake face of the tool.

The predicted temperatures were compared both with the distribution provided by thermography (Fig. 12) and with the local measurements provided by the thermocouples.

The comparison supplied good results, in steady-state conditions, even if the FEM tends to overestimate the temperatures of about 20%.

It is worth pointing out that the numerical values depend on the incoming thermal flux indeed, apart a suitable calculation of the mechanical power quota, the temperature predictive capability increases, as compared to the one furnished by the thermo-mechanical simulation.

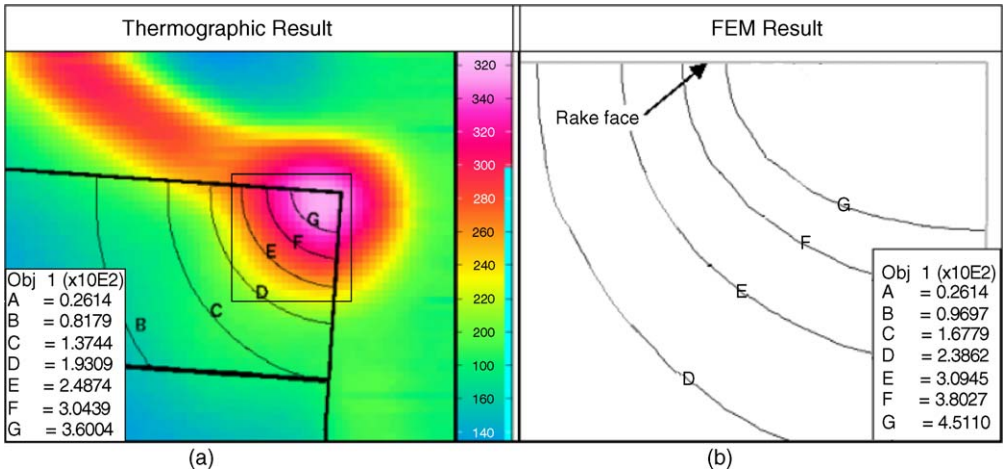


Fig. 12. Case $V = 200$ m/min, $f = 0.2$ mm/rev: (a) experimental results and (b) numerical results.

## 4. Discussion

Accurate prediction of the temperature fields in the tool is necessary, since it provides precious information to model some interesting phenomena which occur on the tool. Wear is just the most relevant one, due to the heavy implications on tool life, then on process costs, and machined product quality.

Numerical simulation is a very powerful tool and many FE codes are able to develop coupled simulations.

Unfortunately, as far as temperature prediction is concerned, the simulated cutting length at conventional cutting speeds is not sufficient to permit the achievement of steady-state conditions, even if a simplified 2D simulation is run.

Thus, it is necessary to move research focus toward two directions:

1. the development of most efficient FE codes, allowing a very large number of elements, running on high performance multiprocessor computers;
2. the use of hybrid simulations in which steady-state is reached through a pure thermal analysis, providing as input data the thermal and mechanical actions on the tool rake face.

In the opinion of the authors, the first line may be pursued in a medium period time, according to the current development trend.

On the other hand, in the next few years, the second line has to be carefully explored: first results may be recognised [20] in literature but new research efforts have to be surely spent in this direction in order to obtain new and significant results from FE numerical simulation of machining processes.

## 5. Conclusions

The thermal field in an orthogonal cutting process has been investigated utilizing both a punctual technique, based on the use of thermocouples, and a "whole field" methodology, using a thermocamera. At the end of the above analysis, some conclusions can be drawn:

- Different measuring techniques have to be integrated for obtaining consistent data in temperature revealing due to the complexity of machining processes.
- The use of numerical simulation for predicting temperatures today supplies partial data, due to the high computational time required for correct simulation.
- For some applications, the use of fully 3D static simulation can be suitable. Obviously, in these cases, the right set-up of the boundary conditions becomes the most critical aspects.

## Acknowledgement

This research is funded by the Italian Ministry of University and Scientific Research (MIUR).

## References

[1] M.C. Shaw, Metal Cutting Principles, Oxford University Press, 1984.
[2] G. Boothroyd, Fundamentals of Machining and Machine Tools, 2nd ed., Marcel Dekker, 1989.
[3] S. Kalpakjian, Manufacturing Processes for Engineering Materials, 3rd ed., Addison-Wesley, 1997.
[4] E.M. Trent, P.K. Wright, Metal Cutting, 4th ed., Butterworths/Heinemann, 2000.
[5] G. Boothroyd, Photographic technique for the determination of metal cutting temperatures, Br. J. Appl. Phys. 12 (1961) 309–324.
[6] B.T. Chao, H.L. Li, K.J. Trigger, An experimental investigation of temperature distribution at tool-flank surface, Trans. ASME 83 (1961) 496–504.
[7] O.D. Prins, The influence of wear on the temperature distribution at the rake face, Ann. CIRP XVIV (1971) 579–584.
[8] P. Lezanski, M.C. Shaw, Tool face temperatures in high speed milling, Trans. ASME 112 (1990) 132–135.
[9] H. Ay, W.J. Yang, J.A. Yang, Dynamics of cutting tool temperatures during cutting process, Exp. Heat Transfer 7 (1994) 203–216.
[10] D.A. Stephenson, Assessment of steady-state metal cutting temperature models based on simultaneous infrared and thermocouple data, ASME J. Eng. Ind. 113 (1991) 121–128.
[11] P. Muller-Hummen, M. Larhes, J. Mehlhose, G. Lang, Measurement of temperature in diamond coated tools during machining processes, Diamond Film Technol. 7 (1997) 219–239.
[12] R. M'Saoubi, C. La Calvez, B. Changeaux, J.L. Lebrun, Thermal and microstructural analysis of orthogonal cutting of a low alloyed carbon steel using an infrared-charge-coupled device camera technique, Proc. Inst. Mech. Eng. 216 (2002) 153–165.
[13] M.A. Davies, A.L. Cooke, E.R. Larsen, High bandwidth thermal microscopy of machining AISI 1045 Steel, Ann. CIRP (54/1) (2005).
[14] M.A. Davies, Q. Cao, A.L. Cooke, R. Ivester, On the measurement and prediction of the temperature fields in machining AISI, Ann. CIRP (52) (2003).
[15] M.R. Miller, G. Mulholland, C. Anderson, Experimental cutting tool temperature distributions, ASME J. Manuf. Sci. Eng. 125 (4) (2003) 667–673.
[16] Y.K. Potdar, A.T. Zehnder, Measurements and simulations of temperature and deformation fields in transient metal cutting, ASME J. Manuf. Sci. Eng. 125 (2003) 645–655.
[17] V.P. Astakhov, Metal Cutting Mechanics, CRC Press, 1999.
[18] Z.C. Lin, S.Y. Lin, A coupled finite element model of thermo-plastic large deformation for orthogonal cutting, J. Eng. Mater. Technol. 114 (1992) 218–226.
[19] E. Ceretti, L. Filice, F. Micari, Basic aspects and modeling of friction in cutting, Int. J. Forming Process. 4 (1/2) (2001) 73–87.
[20] Y.C. Yen, J. Sohner, B. Lilly, T. Altan, Estimation of tool wear in orthogonal cutting using the finite element analysis, J. Mater. Process. Technol. 146 (2004) 82–91.